Choosing a proper complete active space in calculations for transition metal dimers: ground state of Mn_2 revisited†

Cristopher Camacho,[a] Shigeyoshi Yamamoto[b] and Henryk A. Witek*[a]

Received 26th March 2008, Accepted 21st May 2008
First published as an Advance Article on the web 24th June 2008
DOI: 10.1039/b805125a

The potential energy curve of the ground state of Mn_2 has been studied using a systematic sequence of complete active spaces. Deficiencies of the routinely used active space, built from atomic 4s and 3d orbitals, has been identified and discussed. It is shown that an additional σ_g orbital, originating from the atomic virtual $4p_z$ orbitals, is essential for a proper description of static correlation in the $^1\Sigma_g^+$ state of Mn_2. The calculated spectroscopic parameters of the $^1\Sigma_g^+$ state agree well with available experimental data. The calculated equilibrium bond lengths are located between 3.24 and 3.50 Å, the harmonic vibrational frequencies, between 44 and 72 cm^{-1}, and the dissociation energies, between 0.05 and 0.09 eV. An urgent need for an accurate gas-phase experimental study of spectroscopic constants of Mn_2 is highlighted.

I. Introduction

The choice of an appropriate active space in the complete active space self-consistent field (CASSCF) calculations can pose a difficult practical problem for many molecular systems. The most natural choice—of a full valence space containing all valence electrons and all valence orbitals—is applicable only to very simple molecules. For larger systems, it is necessary to select a set of chemically important orbitals that describe correctly the chemical character of a given electronic state. An appropriate choice of CAS can be particularly difficult in cases where smooth and continuous potential energy surfaces (PES) corresponding to some specific molecular processes, like dissociation or chemical reaction, are sought.

The most obvious choice of active space for calculating potential energy curves of the manganese dimer is the full valence space, comprising the 4s, 3d, and 4p orbitals of each of the metal atoms. Unfortunately, this choice is infeasible owing to the prohibitively large size of the resulting CASSCF problem. Correlating 14 active electrons in 18 active orbitals produces more than 200 million configuration state functions (CSF) with singlet spin symmetry; point group symmetry allows to reduce this number to approximately 25 million CSFs. At present, the largest reported dimension of the CASSCF problem[1] is approximately equal to 9 millions. This study—that can be described as state of the art in this field—was performed for the low-lying states of SiC_3 and correlated 16 electrons in 16 active orbitals, which lead to approximately 35 million CSFs distributed over four irreducible representations of the C_{2v} point group. A generally accepted belief in the computational chemistry community is that 16 active orbitals may be the limit at the present stage of development of computer technology. It is possible that the recent developments[2–4] in density matrix renormalization group (DRMG) can help remove this limitation. Unfortunately, this method is not yet widely available and, therefore, to study the low-lying states of manganese dimer, a reduced valence space is usually introduced. Most of the reported multiconfigurational SCF calculations on transition metal dimers employ some complete or restricted active space[5–25] that is constructed with only the 4s and 3d (or, more generally, *n*s and $(n-1)$d) orbitals of each metal atom. To our best knowledge, there are only two publications using a larger number of active orbitals for this type of calculations. Roos[26] has reported calculations of the ground state of the chromium dimer using 12 active electrons distributed among 16 active orbitals. The number of CSFs in this study is approximately equal to 1.8 million. The other study is the publication of Suzuki and his coworkers on low-lying states of the scandium dimer.[27] They were able to correlate six valence electrons of Sc_2 into as many as 22 active orbitals, which yielded a complete active space spanned by 16 122 CSFs. Here, crossing the limit of 16 active orbitals was only possible because of a very limited number of active electrons. The 22 active orbitals in this study originated from the 4s, 3d, and 4d orbitals of the separated atoms.

Recently, Yamamoto *et al.*[28] have reported accurate multireference calculations of the low-lying states of the manganese dimer using a reduced valence space composed of the 4s and 3d orbitals of both Mn atoms. Three electronic states of Mn_2 ($^1\Sigma_g^+$, $^{11}\Sigma_u^+$, and $^{11}\Pi_u$) have been studied using CASSCF and second-order multiconfigurational quasidegenerate perturbation theory (MCQDPT). The lowest of them was found to be $^1\Sigma_g^+$ and it was concluded that it is the ground state of Mn_2. The bound character of the $^1\Sigma_g^+$ PES is recovered only after including dynamic correlation at the MCQDPT level. The calculated spectroscopic parameters corresponded well to the available experimental data.[29,30] The results obtained by Yamamoto *et al.* are consistent with another multireference

[a] *Institute of Molecular Science and Department of Applied Chemistry, National Chiao Tung University, 1001 Ta-Hsueh Road, Hsinchu, 30010, Taiwan. E-mail: hwitek@mail.nctu.edu.tw*
[b] *Faculty of Liberal Arts, Chukyo University, 101-2 Yagoto-Honmachi, Showa-ku, Nagoya, Aichi, 466-8666, Japan*

† Electronic supplementary information (ESI) available: Additional computational details and results. See DOI: 10.1039/b805125a

perturbation study of Mn_2 performed by Wang and Chen[31] that used the same reduced valence space. Note that a systematic multireference configuration interaction (MRCI) study of the ground state of Mn_2 is not probably possible if one wants to use the CASSCF reference wave function. The MRCI calculations performed by us using the CAS + DDCI module of the COST program[32] with the (10o,10e) CASSCF reference wave function yield a repulsive curve. This calculation uses over 48 million Slater determinants. It is possible that enlarging CAS would yield a bound MRCI curve, but such a MRCI calculation would be prohibitively expensive. Similar observation was made earlier for Cr_2,[33] where even crossing the limit of one billion CSFs could not reproduce accurate spectroscopic parameters. For now, the multireference perturbation theory offers the only way to estimate the ground state PES of Mn_2.

In the present study we perform a systematic study of various active spaces applicable for multireference perturbation theory calculations on the ground state of Mn_2. We are not aware of any other systematic study that would provide deeper insight on the dependence of the quality of calculated potential energy surfaces on the truncation of the full valence space. We believe that our results can be useful also for other transition metal dimers and various related systems.

II. Computational details

The potential energy surface of the $^1\Sigma_g^+$ ground state of Mn_2 has been studied with second-order single-state multireference Møller–Plesset (MRMP) perturbation theory[34,35] using a systematic sequence of various active spaces. Eight different complete active spaces have been explicitly considered. The starting point for constructing these active spaces is the reduced active space that was previously employed by other groups.[7,28,31,36] This active space consists of 14 electrons correlated in 12 orbitals; we denote it concisely as (12o,14e), where 12o stands for 12 active molecular orbitals and 14e stands for 14 active electrons. Detailed description of active orbitals in each of the active spaces is given in Table 1 together with the size of the resulting CASSCF problem, which is defined as a number of singlet CSFs with the A_g symmetry.[37] The calculations using the five smaller active spaces have been carried out using the graphical unitary group CSFs code,[35,38] while the calculations for the remaining active spaces have been performed with the determinant full configuration-interaction code[39] implemented in the GAMESS[40] molecular electronic structure program. The all-electron Gaussian-type basis set contracted as (18s15p8d4f2g)/[7s6p4d4f2g] has been taken from a previous study.[28] Small BSSE corrections (see below) suggest that no serious improvement can be expected upon enlarging the basis set. Similar conclusion can be reached after checking the $^1\Sigma_g^+$ spectroscopic parameters derived from the (13o,14e) CASSCF potential energy curves computed using the Douglas–Kroll augmented correlation consistent polarized valence triple- and quadruple-zeta basis sets of Peterson.[41,42] The values of the spectroscopic parameters derived with these three basis sets (r_e = 3.56 Å, ω_e = 60 cm^{-1}, D_e = 0.15 eV) are similar to those obtained with the basis set employed in the present study (r_e = 3.53 Å, ω_e = 66 cm^{-1}, D_e = 0.14 eV). Note that the calculations using the Peterson basis sets employ also the third-order Douglas–Kroll Hamiltonian, which shows that the relativistic correction can be neglected in the present study. The 1s, 2s and 2p orbitals of each manganese atom are not correlated in the MRMP calculations. No additional intruder state avoiding techniques[43] are used since the intruders appear only at very short distances. The basis set superposition error has been estimated using the standard counterpoise correction approach[44,45] using two limiting atomic cases: the full (9o,7e) and the reduced (6o,7e) valence atomic active spaces. The BSSE corrections computed with both procedures are small (<0.1 mH for CASSCF and <2.0 mH for MRMP). The MRMP non-size consistency error is also found to be small (<0.1 mH). More systematic discussion of possible computational errors and additional details of our calculations are given in the ESI.†

III. Results

A Choice of active space

The routinely used (12o,14e) reduced valence space is composed of the 4s and 3d orbitals of each of the Mn atom.[46] Unfortunately, such a choice of an active space in the calculations on the ground state of Mn_2 leads to a discontinuity in the computed MRMP and CASSCF potential energy curves approximately at 4.23 Å (see Fig. 1). The discontinuity originates from the 4s ↔ 3p orbital switch between the active and doubly occupied CAS subspaces. The switch is only possible because all the involved molecular orbitals are effectively doubly occupied. A detailed discussion of this phenomenon is given in the ESI† accompanying this paper. One way of avoiding the discontinuity problem, used in the previous study[28] of the $^1\Sigma_g^+$ state of Mn_2, is to perform state-averaging in the CASSCF calculations. The first excited state of the manganese dimer corresponds to a transfer of a single electron from 4s into 3d. A set of MOs averaged

Table 1 Definition of complete active spaces used for the CASSCF calculations. The dimension of each space is given in the last column

Active space	Orbitals										CSFs
(12o,14e)	$\sigma_g^{(4s)}$	$\sigma_u^{(4s)}$	$\sigma_g^{(3d)}$	$\sigma_u^{(3d)}$	$\pi_g^{(3d)}$	$\pi_u^{(3d)}$	$\delta_g^{(3d)}$	$\delta_u^{(3d)}$			21 588
(12o,12e)		$\sigma_u^{(4s)}$	$\sigma_g^{(3d)}$	$\sigma_u^{(3d)}$	$\pi_g^{(3d)}$	$\pi_u^{(3d)}$	$\delta_g^{(3d)}$	$\delta_u^{(3d)}$	$\sigma_g^{(4p)}$	$\sigma_u^{(4s)}$	28 784
(13o,12e)[1]		$\sigma_u^{(4s)}$	$\sigma_g^{(3d)}$	$\sigma_u^{(3d)}$	$\pi_g^{(3d)}$	$\pi_u^{(3d)}$	$\delta_g^{(3d)}$	$\delta_u^{(3d)}$	$\sigma_g^{(4p)}$	$\sigma_g^{(5s)}$	92 978
(13o,12e)[2]		$\sigma_u^{(4s)}$	$\sigma_g^{(3d)}$	$\sigma_u^{(3d)}$	$\pi_g^{(3d)}$	$\pi_u^{(3d)}$	$\delta_g^{(3d)}$	$\delta_u^{(3d)}$	$\sigma_g^{(4p)}$	$\sigma_u^{(4p)}$	92 978
(13o,14e)	$\sigma_g^{(4s)}$	$\sigma_u^{(4s)}$	$\sigma_g^{(3d)}$	$\sigma_u^{(3d)}$	$\pi_g^{(3d)}$	$\pi_u^{(3d)}$	$\delta_g^{(3d)}$	$\delta_u^{(3d)}$	$\sigma_g^{(4p)}$		92 978
(14o,12e)		$\sigma_u^{(4s)}$	$\sigma_g^{(3d)}$	$\sigma_u^{(3d)}$	$\pi_g^{(3d)}$	$\pi_u^{(3d)}$	$\delta_g^{(3d)}$	$\delta_u^{(3d)}$	$\sigma_g^{(4p)}$	$\pi_u^{(4p)}$	269 665
(14o,14e)	$\sigma_g^{(4s)}$	$\sigma_u^{(4s)}$	$\sigma_g^{(3d)}$	$\sigma_u^{(3d)}$	$\pi_g^{(3d)}$	$\pi_u^{(3d)}$	$\delta_g^{(3d)}$	$\delta_u^{(3d)}$	$\sigma_g^{(4p)}$	$\sigma_u^{(4p)}$	347 360
(15o,14e)	$\sigma_g^{(4s)}$	$\sigma_u^{(4s)}$	$\sigma_g^{(3d)}$	$\sigma_u^{(3d)}$	$\pi_g^{(3d)}$	$\pi_u^{(3d)}$	$\delta_g^{(3d)}$	$\delta_u^{(3d)}$	$\sigma_g^{(4p)}$	$\pi_u^{(4p)}$	1 153 200

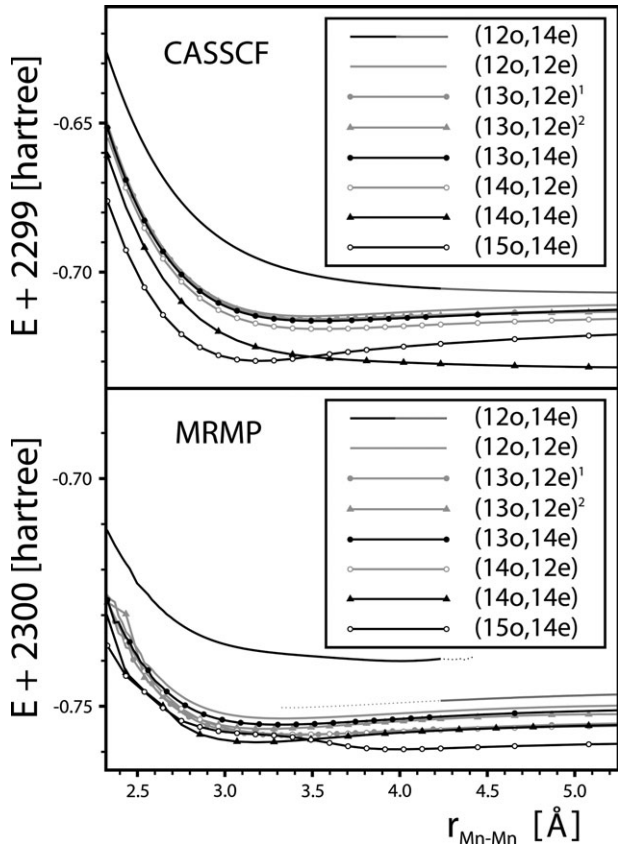

Fig. 1 The CASSCF and MRMP potential energy curves or the $^1\Sigma_g^+$ state of Mn_2 calculated using the (12o,14e), (12o,12e), (13o,12e)^1, (13o,12e)^2, (13o,14e), (14o,12e), (14o,14e), and (15o,14e) active spaces. For (12o,14e), the dotted lines correspond to semistable solutions at short and long distances.

over the ground and the first excited states yields the occupation numbers smaller than two for the σ_g and σ_u MOs constructed from the atomic 4s AOs and prevents their mixing with inactive orbitals. Another way of stabilizing the long-distance solution at shorter distances is to add an additional virtual σ_g orbital to the active space. Augmenting the active space with such an orbital stabilizes the correct solution at shorter distances by effective lowering of the occupation number for the $\sigma_u^{(4s)}$ (and possibly $\sigma_g^{(4s)}$) orbitals. The addition of one extra σ_g virtual MO to the (12o,14e) active space turns out to play also an essential role in the correct description of static correlation for the Mn_2 ground state wave function. As we show later (see Fig. 2), the additional $\sigma_g^{(4p_z)}$ orbital is the only virtual MO that has non-negligible occupation number when added to the active space. The augmented active space—denoted as (13o,14e)—contains 14 electrons distributed over 13 active orbitals. Another useful information obtained from Fig. 2 is the closed-shell character of the $\sigma_g^{(4s)}$ orbital over the whole PES. This observation suggests that this orbital can be safely included in the doubly-occupied space without deteriorating the quality of results. As anticipated, the resulting active space, denoted as (12o,12e), displays very similar characteristic to the (13o,14e) active space but simultaneously allows for significant savings in computational time.

It is natural to ask if including further virtual orbitals in the active space would improve significantly the description of the ground state wave function. The plausible candidates to be included in the active space are: the bonding π_u orbitals originating from the 4p AOs, the bonding σ_g orbital originating from the 5s AOs, and the antibonding σ_u orbital originating from the 4p AOs. All the resulting active spaces considered by us explicitly in this study are listed in Table 1. It is clear from Fig. 2 that including further virtual orbitals in the active space modifies neither the natural orbitals occupation patterns nor the orbital energies to a large degree. The occupation numbers corresponding to the extra π_u, σ_g, and σ_u active orbitals are negligible over the whole potential energy curve. It is interesting to see from Fig. 1 that the studied modifications of the active space have crucial effect on the shape of the calculated PESs at the CASSCF level. Note that this arbitrariness partially vanishes after accounting for dynamical correlation; the calculated MRMP curves shown in Fig. 1 have rather similar characteristics.

B Bonding mechanism in Mn_2

The wave function of the $^1\Sigma_g^+$ state of Mn_2 is found to be truly multiconfigurational as signalized earlier by Bauschlicher.[36] The leading CSF, which corresponds to the closed-shell Slater determinant, contributes only 0.5% to the wave function at the equilibrium geometry. This value is spectacularly smaller than 45% obtained[26] for the HF-like configuration in the ground state of Cr_2, which is considered to be a representative example of a multiconfigurational wave function. The difference of magnitude between these two values may illustrate the scale of difficulty corresponding to a proper description of the Mn_2 ground state wave function and at the same time explain the complete failure of the density functional theory.[47–49] A very detailed, distance-dependent analysis of the $^1\Sigma_g^+$ wave function is presented in the ESI.†

To understand the nature of the chemical bond in the $^1\Sigma_g^+$ state of Mn_2 we analyze the orbital energies[50] and occupation numbers for the active orbitals in the CASSCF calculations. They are shown in Fig. 2. The bonding contribution from the 3d AOs is negligible except for very short distances. Thus, the $^1\Sigma_g^+$ wave function corresponds to a highly multiconfigurational, open-shell singlet state with ten unpaired 3d electrons. For all the considered active spaces, the bond order—defined in a standard way as a half of the difference between the number of electrons in bonding and antibonding orbitals—is smaller than 0.5 except for distances below 2.6 Å. (For details, see Fig. S10 of the ESI.†) No information on the bonding mechanism can be inferred from the shape of the CASSCF potential energy curves calculated with various active spaces (see Fig. 1). This example shows that for weakly bound molecules, like Mn_2, the CASSCF method may give almost arbitrary information about the shape of the ground state potential energy curves owing to a very delicate balance between the bonding and antibonding character of the active orbitals. Similar effect was observed previously for Cr_2,[13,26,51] Be_2,[52] and high-spin states of Mn_2.[53] The calculated MRMP potential energy curves—except for the (12o,14e) and (15o,14e) PESs—show that the equilibrium bond distance in

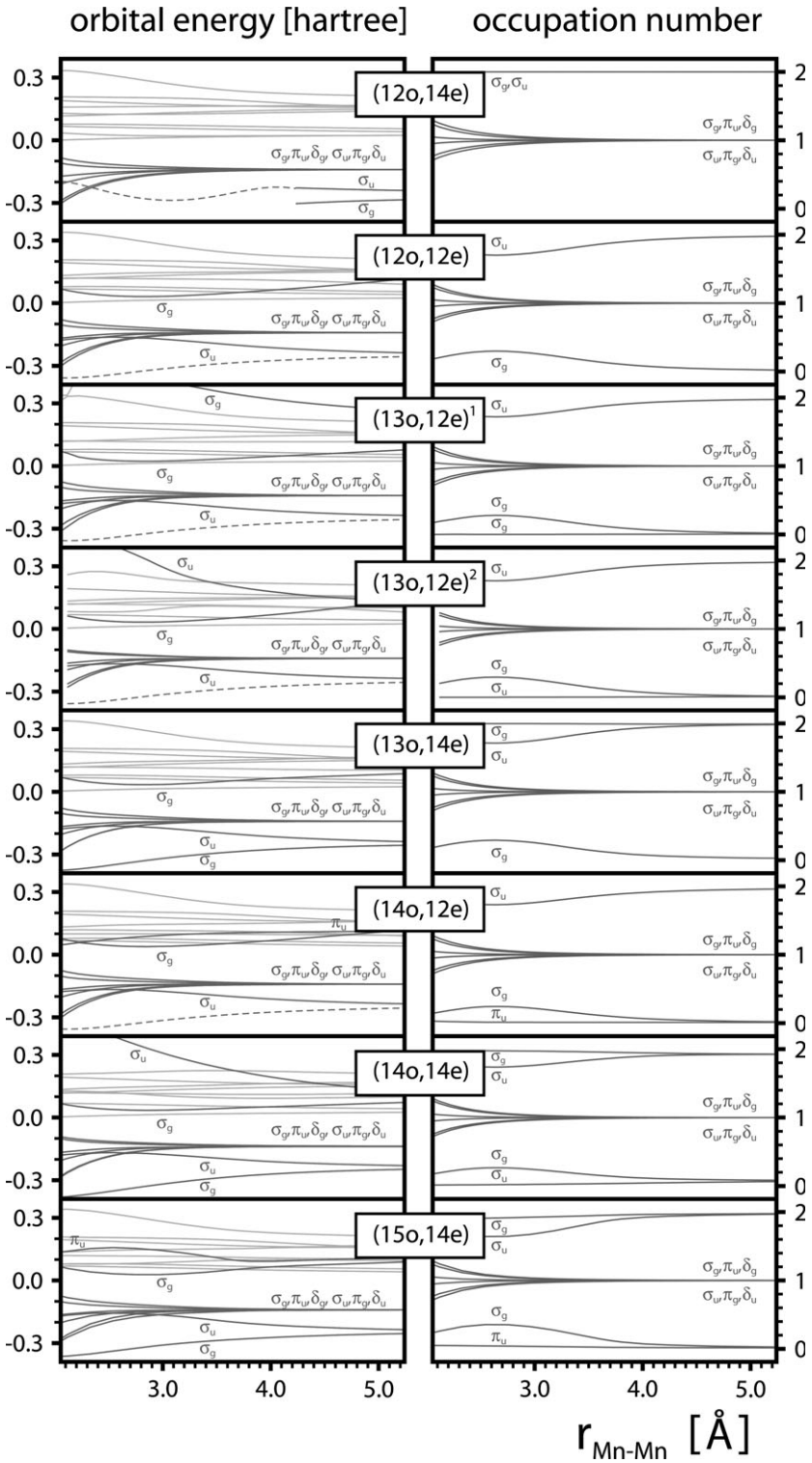

Fig. 2 One-electron energies[50] (left panel) and occupation numbers (right panel) of the canonical active orbitals calculated for all the considered active spaces. The orbital energies of active orbitals (solid black) are shown together with analogous data for inactive (dashed line) and virtual (solid gray) orbitals.

Mn_2 is approximately equal to 3.3 Å. The calculated dissociation energy ($\approx$0.1 eV) corresponds clearly to a weakly bound molecule, presumably to a van der Waals complex.

The van der Waals character of Mn_2 is also indicated by our other findings: (i) repulsive character of the CASSCF curves obtained with the well-balanced (12o,14e) and (14o,14e) active spaces, (ii) chemically inactive character of the 4d atomic orbitals, (iii) negligible bond order at the CASSCF level, and (iv) the closed-shell character of the σ_g originating from the 4s AOs. All closed-shell metals (Be, Mg, *etc.*) and noble gases

(He, Ne, *etc.*) display similar CASSCF behavior[52,54–59] for the simple reason that dispersion attraction—practically the only binding force there—is never fully recovered by valence-space CASSCF calculations. Extending the reduced valence space with a single virtual σ_g orbital brings about some attraction directly related to the dipole–dipole dispersion interaction, yet it is only some fraction of total dispersion, inadequate to grasp quantitatively the magnitude of van der Waals binding. This observation is further corroborated by augmenting the valence space with additional π_u orbital, which brings about more dispersion leading to a deeper PES and shorter equilibrium bond length. On the other hand, adding an additional σ_u orbitals results in better description of the multireference character of Mn_2 and allows for recovering a larger portion of the intra-atomic correlation. These two effects compete in producing the large arbitrariness observed in the shape of calculated CASSCF potential energy curves. The unbound form of the (12o,14e) and (14o,14e) CASSCF curves suggests that also the full valence PES is repulsive. Since the (18o,14e) CASSCF calculations are beyond our reach at the moment, we test this hypothesis using the occupation-restricted multiple active spaces (ORMAS) approach[60,61] implemented in the GAMESS program.[40] The ORMAS estimations of the (18o,14e) CASSCF potential energy curve indeed show an unbound shape. Technical details of these calculations are given in the ESI.†

C Spectroscopic constants

The CASSCF and MRMP spectroscopic constants of the $^1\Sigma_g^+$ state of Mn_2 calculated using all the considered complete active spaces are displayed in Table 2. To illustrate the influence of the basis set superposition error (BSSE) corrections on the results, the spectroscopic parameters derived from the original and BSSE-corrected curves are shown together. For CASSCF, the BSSE corrections are negligible. For MRMP, the changes are somewhat larger; the BSSE-corrected equilibrium bond lengths are longer by 0.07–0.10 Å, the harmonic vibrational frequencies are smaller by 3–7 cm^{-1}, and the dissociation energies are smaller by 0.01–0.02 eV. The spectroscopic parameters could be computed for all potential energy surfaces except for the (12o,14e) and (14o,14e) CASSCF curves (repulsive PESs), the (12o,14e) MRMP curve (discontinuous PES), and the (15o,14e) MRMP curve (strongly perturbed PES; see ESI† for detailed discussion).

The calculated MRMP equilibrium bond distances are located between 3.24 and 3.50 Å. These values correspond well to the previously published MCQDPT value[28] of 3.29 Å and to the experimental value[62] of 3.4 Å. The experimental value was derived indirectly from electron spin resonance measurements for higher-spin states of the manganese dimer trapped in a solid krypton matrices. No experimental data for the gas-phase Mn_2 are available. The calculated MRMP harmonic vibrational frequencies are located between 44 and 72 cm^{-1}. These values correspond well to the previously calculated MCQDPT result[28] of 54 cm^{-1}. No gas-phase experimental harmonic vibrational frequency is available for the $^1\Sigma_g^+$ state of Mn_2. However, the calculated MRMP values of ω_e agree well with the harmonic vibrational frequency of the matrix-isolated Mn_2: 68 cm^{-1} in a solid xenon matrix,[30] 76 cm^{-1} in a solid krypton matrix,[29] and 59 and 68 cm^{-1} at two different sites of a solid argon matrix.[29] The dissociation energy D_e calculated using MRMP is located between 0.05 and 0.09 eV. The previously published MCQDPT value was equal to 0.14 eV. The experimental value was estimated[63] to be 0.13 ± 0.13 eV. More recent estimations show that D_e is between 0.02 and 0.15 eV.[64] Summarizing, we can say that all the calculated MRMP spectroscopic constants correspond rather well to the available experimental data.

IV. Discussion

A deeper analysis of available experimental data suggests that in fact very little is known about the spectroscopic properties of the $^1\Sigma_g^+$ state of Mn_2. The previous and current theoretical estimates of the spectroscopic parameters seem to support the validity of experimental data. However, virtually all the experimental data were obtained for Mn_2 trapped in solid rare-gas matrices. Since the manganese dimer is a weakly bound van der Waals complex, its molecular properties can

Table 2 Spectroscopic constants of the $^1\Sigma_g^+$ state of Mn_2 calculated using the BSSE-corrected CASSCF and MRMP methods. Values without BSSE corrections are given in parentheses. The bond distances r_e are given in Å, the dissociation energies D_e, in eV, and the harmonic vibrational frequencies ω_e, in cm^{-1}

	CASSCF			MRMP		
Active space	r_e	ω_e	D_e	r_e	ω_e	D_e
(12o,14e)	—[a]	—[a]	—[a]	—[b]	—[b]	—[b]
(12o,12e)	3.48 (3.48)	74 (73)	0.12 (0.12)	3.42 (3.33)	52 (55)	0.08 (0.09)
(13o,12e)[1]	3.54 (3.53)	68 (65)	0.09 (0.09)	3.44 (3.34)	50 (54)	0.07 (0.09)
(13o,12e)[2]	3.53 (3.53)	67 (67)	0.08 (0.08)	3.30 (3.25)	62 (67)	0.09 (0.10)
(13o,14e)	3.54 (3.53)	67 (66)	0.14 (0.14)	3.38 (3.31)	54 (58)	0.08 (0.10)
(14o,12e)	3.55 (3.55)	68 (68)	0.11 (0.11)	3.50 (3.41)	44 (49)	0.05 (0.06)
(14o,14e)	—[a]	—[a]	—[a]	3.24 (3.17)	72 (79)	0.09 (0.11)
(15o,14e)	3.19 (3.19)	120 (120)	0.25 (0.25)	—[c]	—[c]	—[c]
MCQDPT[d]	—[a]	—[a]	—[a]	3.29	53	0.14
CASPT2[e]	—[a]	—[a]	—[a]	3.64	—[f]	0.12
Exp.	r_e = 3.4[g]	ω_e = 68,[h] 76,[i] 59,[j] 68[j]	D_e = 0.13 ± 0.13[k]			

[a] Repulsive PES. [b] Discontinuous PES. [c] The shape of PES does not allow for simple determination of spectroscopic parameters. [d] Ref. 28. No BSSE correction considered. [e] Ref. 31. No BSSE correction considered. [f] No data available. [g] Ref. 62. [h] In xenon matrix, ref. 30. [i] In krypton matrix, ref. 29. [j] At two different sites of the argon matrix, ref. 29. [k] Ref. 63.

depend strongly on the nature of the environment. The best illustration for this is the variation of harmonic vibrational frequency as a function of the noble-gas atoms present in the matrix; the variation is larger than 15 cm^{-1}, which gives the uncertainty of approximately 20%. What would be the value of ω_e of the ground state of the gas phase Mn_2? Is it legitimate to compare our results from the gas-phase calculations with these measurements? Similar controversy concerns the value of the equilibrium bond distance in Mn_2. The commonly accepted experimental value of r_e = 3.4 Å of the $^1\Sigma_g^+$ state of Mn_2 was derived from electron paramagnetic resonance (EPR) measurements for Mn_2 trapped in a krypton matrix.[62] However, a short reflection on this fact reveals that the ground state of Mn_2 has s = 0 and cannot be accessed using the EPR technique. Deeper analysis of ref. 62 shows that the value of 3.4 Å was obtained from axial anisotropic exchange interaction parameter D_e derived from EPR data for higher-spin states (s = 1, 2, 3) of the manganese dimer in the krypton matrix. Therefore, the value of 3.4 Å is only a rough estimate[65] of an effective average bond length of the lowest triplet, quintet, and septet states of Mn_2. The value of D_e derived from the EPR data for other matrices (argon, xenon) would yield a different estimate of this distance. Unfortunately, we are not able to reproduce this effective bond length from the data given in ref. 62. Do these estimates give any information about the singlet states of the manganese dimer? A definitive answer to all the questions posed in this section could only be possible if accurate experimental gas-phase study of spectroscopic parameters of Mn_2 becomes available.

V. Conclusions

A systematic investigation of a series of various active spaces applicable for the CASSCF calculations on the ground state of the manganese dimer has been presented. We have shown that the routinely used (12o,14e) active space built from the atomic 4s and 3d orbitals yields discontinuous CASSCF and MRMP potential energy curves for the $^1\Sigma_g^+$ state of Mn_2. It is demonstrated that augmenting the (12o,14e) active space with a single virtual $\sigma_g^{(4p)}$ orbital improves the situation considerably; the resultant CASSCF and MRMP potential energy curves are continuous. Adding next virtual orbitals to the active space does not modify the $^1\Sigma_g^+$ wave function substantially. In contrast, different choice of active orbitals can lead to an almost arbitrary shape of the CASSCF potential energy curve due to a delicate balance between the bonding and antibonding MOs. This arbitrariness is almost removed after accounting for dynamic correlation; the resultant MRMP curves have a similar shape. Our calculations confirm the highly multiconfigurational character of the $^1\Sigma_g^+$ state of Mn_2. The contribution from the leading Slater determinant at an equilibrium distance is as small as 0.5%. Numerous observations support the van der Waals character of Mn_2: (i) small dissociation energy and long equilibrium bond distance, (ii) inactive character of 3d AOs, (iii) repulsive shape of full valence CASSCF PES, (iv) fractional bond order over the whole PES, and (v) closed shell character of the $\sigma_g^{(4s)}$ MO. It is possible, however, that at short distances (2.4–3.8 Å) there exist strong mixing of configurations corresponding to the two lowest atomic dissociation limits, $4s^23d^5$ + $4s^23d^5$ or $4s^13d^6$ + $4s^23d^5$, that can lead to significant shortening of the equilibrium distance in Mn_2. An indication of such mixing is visible in our (15o,14e) CASSCF and MRMP calculations. We point out this possibility in order to advertise here the need of performing multistate MRPT calculations that would be helpful to clarify this issue.

No experimental gas-phase spectroscopic parameters are available for the manganese dimer. The available experimental data, derived for Mn_2 isolated in noble-gas matrices, display numerous flows. The experimental r_e = 3.4 Å, obtained from the EPR measurements, is computed as an effective average for some triplet, quintet, and septet states of Mn_2. This procedure does not necessarily give any information for the $^1\Sigma_g^+$ state. The experimental dissociation energy D_e = 0.13 eV is characterized by a large relative uncertainty (±100%). Similarly, the experimental vibrational frequency shows large relative dependence on the matrix environment, giving three different values of ω_e: 59, 68, and 76 cm^{-1}. Nevertheless, the computed spectroscopic parameters obtained from the BSSE-corrected MRMP curves correspond well to the available experimental data. The calculated MRMP equilibrium bond lengths are located between 3.24 and 3.50 Å, the harmonic vibrational frequencies, between 44 and 72 cm^{-1}, and the dissociation energies, between 0.05 and 0.09 eV. The BSSE corrections do not influence the computed results to a large degree.

The previous computational study[28] of the ground state of Mn_2 left an impression that its spectroscopic properties have already been fully studied, both in theory and in experiment. The present work casts a shadow on this optimistic picture. Do we really know them? For a definitive answer, we probably have to wait until accurate gas-phase spectroscopic data become available or full-valence active space multistate perturbation theory calculations are feasible.

Acknowledgements

We thank Profs Björn Roos, Grzegorz Chałasiński, Alexei Buchachenko, and Hiroshi Tatewaki for interesting and motivating comments, and Prof. Hélène Bolvin for a copy of the COST program. HAW acknowledges the National Science Council of Taiwan (96-2113-M-009-022-MY3), the Institute of Nuclear Energy Research, the Atomic Energy Council, Taiwan, (contract No. NL940251), and the Ministry of Education (MOE-ATU project) for financial support.

References

1. J. M. Rintelman, M. S. Gordon, G. D. Fletcher and J. Ivanic, *J. Chem. Phys.*, 2006, **124**, 034303.
2. G. K.-L. Chan and M. Head-Gordon, *J. Chem. Phys.*, 2001, **116**, 4462.
3. T. Yanai and G. K.-L. Chan, *J. Chem. Phys.*, 2006, **124**, 194106.
4. D. Ghosh, J. Hachmann, T. Yanai and G. K.-L. Chan, *J. Chem. Phys.*, 2008, **128**, 144117.
5. K. Balasubramanian and X. L. Zhu, *J. Chem. Phys.*, 2001, **114**, 10375.
6. K. Balasubramanian and X. Zhu, *J. Chem. Phys.*, 2002, **117**, 4861.
7. B. Wang and Z. Chen, *J. Chem. Phys.*, 2005, **123**, 134306.
8. T. Noro, C. Ballard, M. H. Palmer and H. Tatewaki, *J. Chem. Phys.*, 1994, **100**, 452.

9. K. K. Das and K. Balasubramanian, *J. Chem. Phys.*, 1991, **95**, 2568.
10. C. Angeli, R. Cimiraglia and J. P. Malrieu, *J. Chem. Phys.*, 2002, **117**, 9138.
11. N. Forsberg and P.-A. Malmqvist, *Chem. Phys. Lett.*, 1997, **274**, 196.
12. K. Andersson, *Chem. Phys. Lett.*, 1995, **237**, 212.
13. B. O. Roos and K. Andersson, *Chem. Phys. Lett.*, 1995, **245**, 215.
14. P. Celani, H. Stoll, H.-J. Werner and P. Knowles, *Mol. Phys.*, 2004, **102**, 2369.
15. O. Hubner and J. Sauer, *Chem. Phys. Lett.*, 2002, **358**, 442.
16. K. Andersson, *Theor. Chem. Acc.*, 2003, **110**, 218.
17. K. Balasubramanian, *Chem. Phys. Lett.*, 2002, **365**, 413.
18. K. Balasubramanian and C. Ravimohan, *J. Chem. Phys.*, 1990, **92**, 3659.
19. K. Balasubramanian and D. W. Liao, *J. Phys. Chem.*, 1989, **93**, 3989.
20. Y. Suzuki, T. Noro, F. Sasaki and H. Tatewaki, *THEOCHEM*, 1999, **461–462**, 351.
21. K. Ellingsen, T. Saue, C. Pouchan and O. Gropen, *Chem. Phys.*, 2005, **311**, 35.
22. X. Cao and M. Dolg, *Theor. Chem. Acc.*, 2002, **108**, 143.
23. I. Itkin and A. Zaitsevskii, *Chem. Phys. Lett.*, 2003, **374**, 143.
24. C. F. Kunz, C. Hättig and B. A. Hess, *Mol. Phys.*, 1996, **89**, 139.
25. A. C. Borin, J. P. Gobbo and B. O. Roos, *Chem. Phys.*, 2008, **343**, 210.
26. B. O. Roos, *Collect. Czech. Chem. Commun.*, 2003, **68**, 265.
27. Y. Suzuki, S. Asai, K. Kobayashi, T. Noro, F. Sasaki and H. Tatewaki, *Chem. Phys. Lett.*, 1997, **268**, 213.
28. S. Yamamoto, H. Tatewaki, H. Moriyama and H. Nakano, *J. Chem. Phys.*, 2006, **124**, 124302.
29. K. D. Bier, T. L. Haslett, A. D. Kirkwood and M. Moskovits, *Chem. Phys. Lett.*, 1988, **89**, 6.
30. A. D. Kirkwood, K. D. Bier, J. K. Thompson, T. L. Haslett, A. S. Huber and M. Moskovits, *J. Phys. Chem.*, 1991, **95**, 2644.
31. B. Wang and Z. Chen, *Chem. Phys. Lett.*, 2004, **387**, 395.
32. N. B. Amor and D. Maynau, *Chem. Phys. Lett.*, 1998, **286**, 211.
33. H. Dachsel, R. Harrison and D. Dixon, *J. Phys. Chem. A*, 1999, **103**, 152.
34. K. Hirao, *Chem. Phys. Lett.*, 1992, **196**, 397.
35. H. Nakano, *J. Chem. Phys.*, 1993, **99**, 7983.
36. C. W. Bauschlicher, Jr, *Chem. Phys. Lett.*, 1989, **156**, 95.
37. We are fully aware that such a choice of active space does not restrict us to the $^1\Sigma_{g+}$ states only, but also includes single components of the Δ_g, Γ_g, and even higher Λ states in CAS. The reason for this inconvenient situation is using the abelian d_{2h} point group in our calculations instead of the full molecular $d_{\infty h}$ point group. An explicit projection onto the $\Lambda = 0$ space is in principle possible (as is done, for example, in the MOLPRO quantum chemistry package) but at present it is not implemented in the GAMESS program.
38. B. R. Brooks and H. F. Schaefer, III, *J. Chem. Phys.*, 1979, **70**, 5092.
39. J. Ivanic and K. Ruedenberg, *Theor. Chem. Acc.*, 2001, **106**, 339.
40. M. W. Schmidt, K. K. Baldridge, J. A. Boatz, S. T. Elbert, M. S. Gordon, J. H. Jensen, S. Koseki, N. Matsunaga, K. A. Nguyen and S. Su, *et al.*, *J. Comput. Chem.*, 1993, **14**, 1347.
41. N. Balabanov and K. Peterson, *J. Chem. Phys.*, 2005, **123**, 064107.
42. N. Balabanov and K. Peterson, *J. Chem. Phys.*, 2006, **125**, 074110.
43. H. A. Witek, Y.-K. Choe, J. P. Finley and K. Hirao, *J. Comput. Chem.*, 2002, **23**, 957.
44. S. F. Boys and F. Bernardi, *Mol. Phys.*, 1970, **19**, 553.
45. J. H. van Lenthe, J. G. C. M. van Duijneveldt-van de Rijdt and F. B. van Duijneveldt, *Adv. Chem. Phys.*, 1987, **69**, 521.
46. It is interesting to note that the van der Waals interactions in the manganese dimer lead to only small perturbation of the atomic structure of each of the Mn atoms. Therefore, it is legitimate to use a twofold way of labelling for the MOs of Mn_2: one using directly the atomic orbitals (*e.g.*, 4s or 3d) and the other one using the in-phase and out-of-phase combinations of AOs (*e.g.*, $\sigma_u^{(4s)}$ or $\sigma_g^{(4p)}$). We use either of these conventions to highlight either atomic or molecular aspects of a given MO.
47. S. K. Nayak and P. Jena, *Chem. Phys. Lett.*, 1998, **289**, 473.
48. S. Yanagisawa, T. Tsuneda and K. Hirao, *J. Chem. Phys.*, 2000, **112**, 545.
49. S. Yamanaka, T. Ukai, K. Nakata, R. Takeda, M. Shoji, T. Kawakami, T. Takada and K. Yamaguchi, *Int. J. Quantum Chem.*, 2007, **107**, 3178.
50. Canonical Fock orbital energies are used. For an exact definition, see eqns (26) and (27) of ref. 35.
51. B. O. Roos, *Acc. Chem. Res.*, 1999, **32**, 137.
52. J. Martin, *Chem. Phys. Lett.*, 1999, **303**, 399.
53. A. A. Buchachenko, private communication.
54. J. Charles, W. Bauschlicher and H. Partridge, *J. Chem. Phys.*, 1984, **80**, 334.
55. L. Rajchel, G. Chałasiński and M. M. Szczesniak, unpublished results.
56. F.-M. Tao, *J. Chem. Phys.*, 1999, **111**, 2407.
57. M. Hanni, P. Lantto, N. Runeberg, J. Jokisaari and J. Vaara, *J. Chem. Phys.*, 2004, **121**, 5908.
58. T. L. Gilbert and A. C. Wahl, *J. Chem. Phys.*, 1967, **47**, 3425.
59. G. Chałasiński, D. J. Funk, J. Simons and W. H. Breckenridge, *J. Chem. Phys.*, 1987, **87**, 3569.
60. J. Ivanic, *J. Chem. Phys.*, 2003, **119**, 9364.
61. J. Ivanic, *J. Chem. Phys.*, 2003, **119**, 9377.
62. C. A. Baumann, R. J. Van Zee, S. V. Bhat and W. Weltner, Jr, *J. Chem. Phys.*, 1983, **78**, 190.
63. A. Kant, S. Lin and B. Strauss, *J. Chem. Phys.*, 1968, **49**, 1983.
64. T. L. Haslett, M. Moskovits and A. Weitzman, *J. Mol. Spectrosc.*, 1989, **135**, 259.
65. J. A. Weil, J. R. Bolton and J. E. Wertz, *Electron paramagnetic resonance: elementary theory and practical applications*, Wiley, New York, 1994.

